Original Article

Coronary computed tomography angiography analysis using artificial intelligence for stenosis quantification and stent segmentation: a multicenter study

Qingtao Meng[1], Pengxin Yu[2]^, Siyuan Yin[2], Xiaofeng Li[2], Yitong Chang[1], Wei Xu[1], Chunmao Wu[1], Na Xu[1], Huan Zhang[2], Yu Wang[2], Hong Shen[2], Rongguo Zhang[2], Qingyue Zhang[2]

[1]Department of Radiology, The Affiliated Chuzhou Hospital of Anhui Medical University, Chuzhou, China; [2]Infervision Medical Technology Co., Ltd., Beijing, China

Contributions: (I) Conception and design: Q Meng, P Yu, R Zhang; (II) Administrative support: None; (III) Provision of study materials or patients: Q Meng, Y Chang, W Xu, C Wu, N Xu; (IV) Collection and assembly of data: Q Meng, Y Chang, W Xu, C Wu, N Xu; (V) Data analysis and interpretation: S Yin, H Zhang, Y Wang, H Shen; (VI) Manuscript writing: All authors; (VII) Final approval of manuscript: All authors.

Correspondence to: Rongguo Zhang, PhD. Infervision Medical Technology Co., Ltd., Tower E, Ocean International Center, Chaoyang District, Beijing 100025, China. Email: zrongguo@infervision.com.

Background: Accurate interpretation of coronary computed tomography angiography (CCTA) is a labor-intensive and expertise-driven endeavor, as inexperienced readers may inadvertently overestimate stenosis severity. Recent artificial intelligence (AI) advances in medical imaging present compelling prospects for auxiliary diagnostic tools in CCTA. This study aimed to externally validate an AI-assisted analysis system capable of rapidly evaluating stenosis severity, exploring its potential integration into routine clinical workflows.

Methods: This multicenter study consisted of an internal and external cohort of patients who underwent CCTA scans between April 2017 and February 2023. CCTA scans were evaluated using Coronary Artery Disease Reporting and Data System (CAD-RADS) scores to determine stenosis severity, while ground-truth stents were manually annotated by expert readers. The InferRead CT Heart (version 1.6; Infervision Medical Technology Co., Ltd., Beijing, China), which incorporates AI-assisted coronary artery stenosis quantification and automatic stent segmentation, was employed for CCTA scan analysis. AI-based stenosis assessment performance was determined using sensitivity, specificity, positive predictive value (PPV), and negative predictive value (NPV), while the AI-based stent segmentation overlap was assessed using the Dice similarity coefficient (DSC).

Results: For ≥50% stenosis diagnoses, the AI system attained per-patient sensitivity, specificity, PPV, and NPV surpassing 90.0% for the internal dataset; for the external dataset, the per-patient values were 88.0% [95% confidence interval (CI): 81.0–94.4%], 94.5% (95% CI: 90.7–97.6%), 90.0% (95% CI: 83.3–95.6%), and 93.4% (95% CI: 89.2–96.8%), respectively. For ≥70% stenosis diagnoses, the per-patient values on the internal dataset were 94.2% (95% CI: 89.2–98.1%), 95.8% (95% CI: 94.1–97.4%), 80.8% (95% CI: 73.5–87.7%), and 98.9% (95% CI: 97.9–99.6%), respectively; for the external dataset, the per-patient values were 91.9% (95% CI: 82.6–100.0%), 97.3% (95% CI: 94.9–99.1%), 85.0% (95% CI: 72.5–94.6%), and 98.6% (95% CI: 96.8–100.0%), respectively. Regarding CAD-RADS categorization, the Cohen kappa was 0.75 and 0.81 for the internal per-patient and per-vessel basis, respectively, and 0.72 and 0.76 for the external per-patient and per-vessel basis, respectively. The DSC for stent segmentation was 0.96±0.06.

Conclusions: The AI-assisted analysis system for CCTA interpretation exhibited exceptional proficiency in stenosis quantification and stent segmentation, indicating that AI holds considerable potential in advancing CCTA postprocessing techniques.

^ ORCID: 0000-0003-4065-0377.

Keywords: Coronary artery disease (CAD); coronary computed tomography angiography (CCTA); coronary artery stenosis; artificial intelligence (AI); deep learning

Submitted Apr 03, 2023. Accepted for publication Aug 30, 2023. Published online Sep 15, 2023.
doi: 10.21037/qims-23-423
View this article at: https://dx.doi.org/10.21037/qims-23-423

Introduction

The Global Burden of Diseases, Injuries, and Risk Factors Study of 2017 identifies cardiovascular disease as a major cause of mortality, accounting for approximately 17.8 million annual deaths and ranking first among noncommunicable diseases, with neoplasms following at 9.6 million deaths (1). Coronary computed tomography angiography (CCTA) has evolved as a potent noninvasive technique for the identification and exclusion of coronary artery disease (CAD) and has demonstrated its efficacy as a primary diagnostic instrument for coronary stenosis (2-5). The introduction of the Coronary Artery Disease Reporting and Data System (CAD-RADS) has streamlined CAD categorization, allowing for the identification of patients who may require further functional testing or invasive angiography (6). Furthermore, the CAD-RADS categorization provides a crucial prognostic function. Xie *et al.* reported that patients with high CAD-RADS scores exhibited significantly increased 5-year event rates compared to those with lower CAD-RADS scores (7). However, accurately assessing stenosis severity using CCTA demands substantial expertise and may involve labor-intensive manual or semiautomated evaluations (8). A substantial 16% discordance in CAD-RADS categorization between on-site and expert readers was observed in a major clinical trial, with on-site readers overestimating severe stenosis (CAD-RADS ≥3) in over 40% of instances (9).

Advancements in artificial intelligence (AI) technology, particularly deep learning, have substantially improved medical image analysis (10). In recent years, AI has been employed to identify coronary stenosis using CCTA scans, aiding clinicians in enhancing diagnostic efficiency and precision in CAD (11-17). Notably, Choi *et al.* (14) were the first to perform external validation of an AI product approved by the USA Food and Drug Administration (FDA) for CCTA-supported analysis, marking a critical milestone in AI's transition from research to clinical practice. Current AI methods typically include coronary stenosis detection, plaque quantification, and classification, with limited focus on coronary stents. As percutaneous coronary intervention (PCI) technology develops, postoperative stent follow-up has become a vital aspect of CCTA (18). In addition to evaluating stent deformation and fracture, addressing in-stent restenosis (ISR) is critical, as it significantly impacts CAD patient prognosis (19). Therefore, automated stent identification is essential for comprehensive AI-based CCTA analysis.

The aim of this study was to externally validate an AI-assisted analysis system (InferRead CTA Coronary version 1.0; Infervision Medical Technology Co., Ltd., Beijing, China) capable of rapidly evaluating stenosis severity and CAD-RADS categorization using CCTA. Additionally, the AI system features automated segmentation for coronary stents, and its performance in this regard was also evaluated. This study will help to improve our understanding of the currently available AI products and their use in clinical practice. We present this article in accordance with the STARD reporting checklist (available at https://qims.amegroups.com/article/view/10.21037/qims-23-423/rc).

Methods

The study was conducted in accordance with the Declaration of Helsinki (as revised in 2013) and was approved by institutional board of The Affiliated Chuzhou Hospital of Anhui Medical University. Individual consent for this retrospective analysis was waived.

Study population

This retrospective, multicenter study included patients from 2 independent cohorts, internal and external. Patients included in the internal cohort hailed from the same center as those utilized for AI system's deep learning model training, yet there was no overlap. Owing to commercial considerations, the internal cohort remains anonymous. The external cohort originated from the Affiliated Chuzhou Hospital of Anhui Medical University and contained data entirely independent from that employed in the AI system's

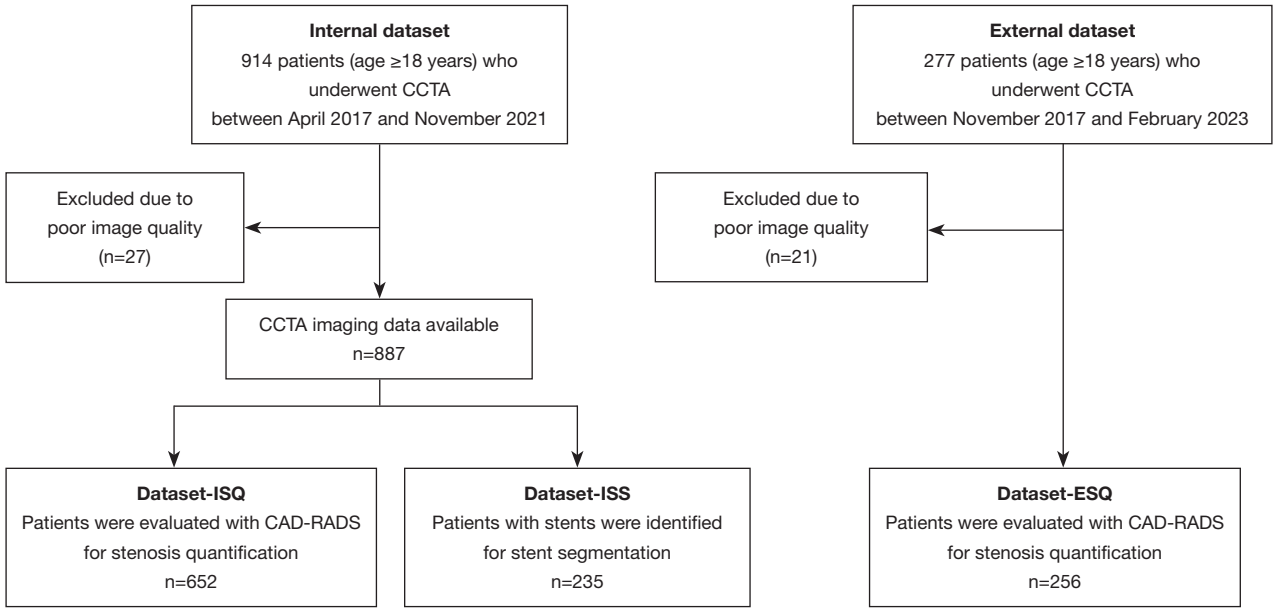

Figure 1 Data exclusion flowchart. This study incorporated 2 independent cohorts. The internal dataset refers to data originating from the same center as the training data used in the deep learning model within the AI system, without overlap. Conversely, the external dataset contains data entirely independent from that employed in the AI system's development. CCTA, coronary computed tomography angiography; ISQ, internal stenosis quantification; ISS, internal stent segmentation; ESQ, external stenosis quantification; CAD-RADS, Coronary Artery Disease Reporting and Data System; AI, artificial intelligence.

development.

We initially included patients aged ≥18 years who had undergone CCTA scans (slice thickness ≤1 mm) between April 2017 and February 2023. Exclusion criteria encompassed CCTA contraindications (such as allergies to iodine contrast agent, unconsciousness, or renal impairment) and poor image quality. According to the exclusion criteria, the internal cohort excluded 27 patients due to poor image quality, and finally 887 patients were enrolled to form a random series; the external cohort excluded 21 patients due poor image quality, and finally 256 patients were enrolled to form a random series (*Figure 1*). CCTA scans from the internal cohort were split into 2 subsets: Dataset-internal stenosis quantification (ISQ) comprised 652 patients and was used for evaluating stenosis quantification performance, and Dataset-internal stent segmentation (ISS) included the remaining 235 patients and was used for evaluating stent segmentation performance. Dataset-external stenosis quantification (ESQ) contained 256 patients from the external cohort. Clinical information for the internal cohort was restricted to gender and age, while additional characteristics for the external cohort were reported if available and included hypertension, dyslipidemia, diabetes, smoking, alcohol, and coronary artery calcium score.

Image acquisition

CCTA scans were acquired using multidetector-row CT scanners from 4 vendors: GE HealthCare (n=251; Chicago, IL, USA), Philips Healthcare (n=172; Amsterdam, the Netherlands), Siemens Healthineers (n=620; Erlangen, Germany), and Toshiba (n=100; Tokyo, Japan). The names, types and parameters of the scanners included in each dataset are detailed in Table S1.

AI-assisted analysis and image analysis

In this study, we validated an AI-assisted analysis system (InferRead CTA Coronary version 1.0; Infervision Medical Technology Co., Ltd.) developed using deep learning for CCTA interpretation support. For each CCTA scan, the process begins with the binary segmentation of coronary arteries, followed by coronary segmental staining, plaque detection, and stent segmentation in 3 mutually independent substeps. The final step of the analysis

involves the quantification of stenosis severity. Initially, the corresponding coronary segment is identified based on each plaque detection result, the relevant segment is then straightened using the centerline of the segment to obtain multiplanar reformatted (MPR) images, and the severity of stenosis is finally calculated based on the MPR. By combining the results of staining and stenosis severity calculation, the severity of stenosis for each coronary segment can be obtained.

Two imaging cardiologists (Xu W with 12 years' experience and Wu C with 10 years' experience) incorporated clinical information, when available, to interpret CCTA scans. In cases of disagreement, a third, expert imaging cardiologist (Meng Q with 20 years' experience) was consulted for the final determination. A visual assessment of each coronary segment, measuring at least 1.5 mm, was conducted, using the 18-segment Society of Cardiovascular Computed Tomography (SCCT) model of the coronary tree (20). Stenosis severity categorization was based on CAD-RADS, with grades evaluated on the following scale of stenosis percentage: 0, absence of stenosis; 1, 1–24%; 2, 25–49%; 3, 50–69%; 4, 70–99%; and 5, 100% (6). The performance analysis in our study focused on the 3 primary vessels: the right coronary artery (RCA), the left main artery with the left anterior descending artery (LM + LAD), and left circumflex artery (LCX). CAD-RADS categories were determined on a per-vessel and per-patient basis, with the highest-grade of stenosis used to establish the category (14).

To evaluate the accuracy of stent segmentation, a manual annotation of the stent region was performed slice by slice on CCTA scans by a junior imaging cardiologist (Chang Y with 3 years' experience) using research software (InferScholar; Infervision Medical Technology Co., Ltd.). The annotation results were further verified and refined by the expert imaging cardiologist (Meng Q) and used as the reference standard for stent segmentation.

Statistical analysis

Continuous variables are presented as the median with interquartile range (IQR), while categorical variables are presented as frequency and percentage.

To evaluate the performance of the AI-based stenosis quantification, assessments were conducted on Dataset-ISQ and Dataset-ESQ for both the per-patient and per-vessel levels. Two thresholds (≥50% and ≥70% of maximal diameter stenosis) were used to compute measures of sensitivity, specificity, positive predictive value (PPV), and negative predictive value (NPV), along with their corresponding confidence intervals (CIs). Bootstrap analysis (1,000 iterations) was employed to estimate the 95% CIs. Additionally, the Cohen kappa coefficient was used to measure the agreement in CAD-RADS categories between the AI-assisted analysis system and the consensus evaluation of the imaging cardiologists.

The degree of overlap between the stent volumes automatically segmented by the AI-assisted analysis system and the stent reference standard was measured using the Dice similarity coefficient (DSC) (21). DSC calculation was performed exclusively for cases where stents were manually identified; that is, Dataset-ISS. Moreover, Bland-Altman analysis with limits of agreement was conducted to assess the concordance between the automatic and manual segmentations of the stent.

A 2-tailed P value <0.05 was considered indicative of a statistically significant difference. All analyses were performed using Python v. 3.8.10 (Python Software Foundation, Delaware, USA) and the libraries numpy v. 1.22.4, scipy v. 1.6.3, sklearn v. 0.24.2, and pandas v. 1.2.4. Based on the sensitivity and specificity values reported by Choi *et al.* (14) and the sample size calculation formula, the minimum sample size was determined to be 204.

Results

Baseline characteristics and analysis time

Dataset-ISQ comprised 652 patients with a median age of 60 years (IQR, 53–68 years), of whom 257 (39.4%) were female. Dataset-ISS included 235 patients with a median age of 63 years (IQR, 56–69 years), and 51 (21.7%) of whom were female. *Table 1* presents the characteristics of the study population for Dataset-ESQ, which consisted of 256 patients with a median age of 60 years (IQR, 52–69 years), of whom 91 (35.5%) were female, 110 (43.0%) had hypertension, 29 (11.3%) had diabetes, 134 (52.3%) had dyslipidemia, 42 (16.4%) were smokers, and 27 (10.5%) were alcohol drinkers.

The AI-assisted analysis system required a median time of 4.97 min (IQR, 4.60–5.42 min) to perform stenosis quantification and stent segmentation, whereas the standard-of-care workflow took radiologists 38.5 min (IQR, 21.7–70.1 min) to draft a report. An example of AI-generated report is shown in Figure S1.

Table 1 Dataset characteristics

Variable	External test dataset (Dataset-ESQ)
Number of cases, n	256
Age (years), median [IQR]	60 [52–69]
Gender, n (%)	
Female	91 (35.5)
Male	165 (64.5)
Hypertension, n (%)	
Yes	110 (43.0)
No	54 (21.1)
Unknown	92 (35.9)
Diabetes, n (%)	
Yes	29 (11.3)
No	126 (49.2)
Unknown	101 (39.5)
Dyslipidemia, n (%)	
Yes	134 (52.3)
No	27 (10.5)
Unknown	95 (37.1)
Smoker, n (%)	
Yes	42 (16.4)
No	124 (48.4)
Unknown	90 (35.2)
Alcohol, n (%)	
Yes	27 (10.5)
No	139 (54.3)
Unknown	90 (35.2)
Coronary artery calcium score, mean ± SD [range]	152±408 [0–3,945]

A portion of the patients originated from outpatient clinics, leading to the presence of incomplete clinical data. EQS, external stenosis quantification; IQR, interquartile range; SD, standard deviation.

Diagnostic performance

Table 2 presents the diagnostic performance of the AI system on both internal and external datasets. In Dataset-ISQ, 41.7% (272/652) of patients exhibited stenosis ≥50%, while 15.8% (103/652) displayed stenosis ≥70%. The AI system's sensitivity and specificity surpassed 90% for both the ≥50% and ≥70% stenosis conditions. For ≥50% stenosis, the AI system's PPV and NPV were 90.6% (95% CI: 87.1–93.9%) and 94.1% (95% CI: 91.6–96.2%), respectively. For ≥70% stenosis, the NPV of the AI system was higher at 98.9% (95% CI: 97.9–99.6%), but the PPV was lower at 80.8% (95% CI: 73.5–87.7%).

Regarding the 3 main vessels, the highest proportion of ≥50% stenosis occurred in LM + LAD (217/652, 33.3%), followed by the LCX (147/652, 22.5%) and the RCA (108/652, 16.7%), accounting for 24.1% (472/1,956) of the total number of vessels. The trend for ≥70% stenosis mirrored that of ≥50% stenosis (LM + LAD: 75/652, 11.5%; LCX: 54/652, 8.3%; RCA: 28/652, 4.3%), accounting for 8.0% (157/1,956) of the total number of vessels. The AI system's sensitivity for both stenosis severities was close to 90%, at 89.2% (95% CI: 86.3–91.8%) for ≥50% stenosis and 89.8% (95% CI: 84.9–94.1%) for ≥70% stenosis.

In the external dataset Dataset-ESQ, stenosis ≥50% was observed in 83.2% (213/256) of patients and 47.7% (366/768) of vessels, while stenosis ≥70% was observed in 35.9% (92/256) of patients and 17.7% (136/768) of vessels. At the per-patient level, the AI system's sensitivity for detecting stenosis ≥50% was 88.0% (95% CI: 81.0–94.4%), and that for detecting stenosis ≥70% was 91.9% (95% CI: 82.6–100.0%).

For the 3 main vessels, the highest proportion of ≥50% stenosis occurred in LM + LAD (76/256, 29.7%), followed by the LCX (31/256, 12.1%) and RCA (29/256, 11.3%). The AI system's sensitivity for ≥50% stenosis vessels was 89.0% (95% CI: 82.7–93.8%). The LM + LAD showed the highest proportion of ≥70% stenosis (26/256, 10.2%), followed by the RCA (15/256, 5.9%) and the LCX (12/256, 4.7%). The AI system's sensitivity for ≥70% stenosis vessels was 86.8% (95% CI: 76.8–95.3%).

CAD-RADS categorization

Figure 2 presents the contingency tables displaying the comparison between AI results and the consensus evaluation of the imaging cardiologists. Dataset-ISQ shows that 81.0% (528/652) of patients demonstrated categorical agreement in CAD-RADS, with 99.7% (650/652) showing agreement within 1 category (*Figure 2A*). The calculated Cohen kappa coefficient was 0.75, indicating a substantial level of agreement between the 2 methods. The most frequent disagreement occurred between AI CAD-RADS 3 and consensus CAD-RADS 2, which was observed in 26 patients

Table 2 Diagnostic performance of AI on a per-patient and per-vessel basis

Dataset	Stenosis	Basis	Sensitivity (%)	Specificity (%)	PPV (%)	NPV (%)
Internal (Dataset-ISQ)	≥50%	Per-vessel (n=1,956)	89.2 (86.3, 91.8)	97.1 (96.2, 98.0)	90.7 (87.9, 93.5)	96.6 (95.6, 97.4)
		Per-patient (n=652)	91.9 (88.3, 94.9)	93.2 (90.7, 95.7)	90.6 (87.1, 93.9)	94.1 (91.6, 96.2)
	≥70%	Per-vessel (n=1,956)	89.8 (84.9, 94.1)	98.4 (97.9, 98.9)	83.4 (77.6, 88.5)	99.1 (98.6, 99.5)
		Per-patient (n=652)	94.2 (89.2, 98.1)	95.8 (94.1, 97.4)	80.8 (73.5, 87.7)	98.9 (97.9, 99.6)
External (Dataset-ESQ)	≥50%	Per-vessel (n=768)	89.0 (82.7, 93.8)	97.3 (96.0, 98.6)	87.7 (81.4, 93.3)	97.6 (96.3, 98.7)
		Per-patient (n=256)	88.0 (81.0, 94.4)	94.5 (90.7, 97.6)	90.0 (83.3, 95.6)	93.4 (89.2, 96.8)
	≥70%	Per-vessel (n=768)	86.8 (76.8, 95.3)	98.6 (97.6, 99.4)	82.1 (69.8, 92.3)	99.0 (98.3, 99.7)
		Per-patient (n=256)	91.9 (82.6, 100.0)	97.3 (94.9, 99.1)	85.0 (72.5, 94.6)	98.6 (96.8, 100.0)

Values in parentheses are 95% confidence intervals. AI, artificial intelligence; PPV, positive predictive value; NPV, negative predictive value; ISQ, internal stenosis quantification; ESQ, external stenosis quantification.

and accounted for 3.9% of the cases. On a per-vessel basis, 85.8% (1,678/1,956) showed categorical agreement in CAD-RADS, with 99.0% (1,937/1,956) demonstrating agreement within 1 category (*Figure 2B*). The calculated Cohen kappa coefficient was 0.81, indicating substantial agreement between the 2 methods. The most frequent disagreement observed was between AI CAD-RADS 1 and consensus CAD-RADS 2, which was found in 53 vessels and accounted for 2.7% of the cases.

Regarding the external dataset Dataset-ESQ, the results showed that 80.1% (205/256) of patients demonstrated categorical agreement in CAD-RADS, with 99.2% (254/256) showing agreement within 1 category (*Figure 2C*). The calculated Cohen kappa coefficient was 0.72, indicating substantial agreement between the 2 methods. The most frequent disagreement occurred between AI CAD-RADS 1 and consensus CAD-RADS 2, which was observed in 13 patients and accounted for 5.1% of the cases. On a per-vessel basis, 83.5% (641/768) demonstrated categorical agreement in CAD-RADS, with 96.2% (739/768) demonstrating agreement within 1 category (*Figure 2D*). The calculated Cohen kappa coefficient was 0.76, indicating a substantial level of agreement between the 2 methods. The most frequent disagreement observed was between AI CAD-RADS 1 and consensus CAD-RADS 0, which was found in 36 vessels and accounted for 4.7% of the cases. Example cases of Dataset-ISQ and Dataset-ESQ were are shown in *Figure 3A*,*3B*, respectively.

Stent segmentation

The AI-assisted analysis system exhibited noninferiority to manual annotation performed by a junior imaging cardiologist concerning stent segmentation performance, with a DSC of 0.96±0.06 compared that of 0.97±0.01 for manual annotation (P=0.44). *Figure 3C* presents representative examples of stent segmentation completed by the AI-assisted analysis system. Bland-Altman analysis (*Figure 4*) revealed a mean difference in DSC between the AI-assisted analysis system and the junior imaging cardiologist of –0.01 (95% CI limits of agreement –0.13 to 0.11).

Discussion

In this multicenter study, we conducted internal and external validation of an AI-assisted analysis system for stenosis quantification and stent segmentation, leveraging CCTA scans.

As a noninvasive examination technique, CCTA plays a vital role in detecting and evaluating CAD. However, the high resolution of CCTA and the complex nature of cardiac structures make stenosis evaluation based on CCTA scans a considerable challenge. Expert imaging cardiologists can attain a semiquantitative estimation of coronary stenosis using the CAD-RADS after meticulous examination over an extended period. However, this process requires significant expertise and is labor-intensive for manual or semiautomated assessments.

AI techniques are being increasingly recognized as valuable tools for improving CCTA postprocessing, as numerous studies have investigated the development of AI algorithms for CCTA analysis. Zreik *et al.* (15) combined convolutional neural networks (CNNs) and recurrent neural networks (RNNs), using 98 CCTA cases for training and

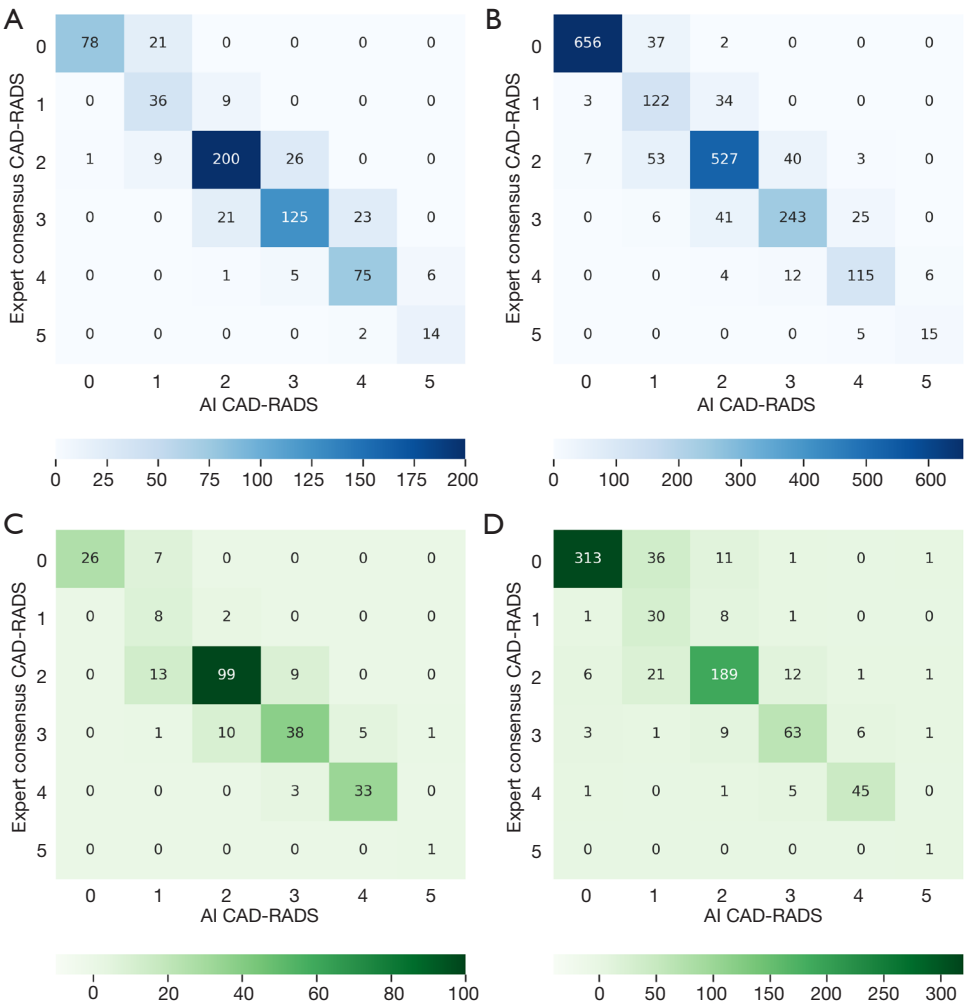

Figure 2 Contingency tables comparing AI-based CAD-RADS scores and the imaging cardiologists' consensus. (A) Per-patient contingency tables in the internal dataset (Dataset-ISQ): the categorical agreement was 81.0% (528/652), while agreement within 1 category reached 99.7% (650/652). The Cohen kappa coefficient was 0.75. (B) Per-vessel contingency tables in Dataset-ISQ: the categorical agreement was 85.8% (1,678/1,956), while agreement within 1 category was 99.0% (1,937/1,956). The Cohen kappa coefficient was 0.81. (C) Per-patient contingency tables in Dataset-ESQ: the categorical agreement was 80.1% (205/256), while agreement within 1 category was 99.2% (254/256). The Cohen kappa coefficient was 0.72. (D) Per-vessel contingency tables in Dataset-ESQ: the categorical agreement was 83.5% (641/768), while agreement within 1 category was 96.2% (739/768). The Cohen kappa coefficient was 0.76. CAD-RADS, Coronary Artery Disease Reporting and Data System; AI, artificial intelligence; ISQ, internal stenosis quantification; ESQ, external stenosis quantification.

68 for testing and achieving an 85% accuracy in detecting significant stenosis (≥50%). Ma *et al.* (22) proposed a transformer-based approach (23) for identifying ≥50% stenosis in CCTA. In contrast to RNN's unidirectional context, the transformer offers increased flexibility in global semantic dependencies, allowing for more effective use of coronary anatomical structure priors. Ma *et al.* reported a 92% accuracy rate with a 76-patient dataset. Muscogiuri *et al.* (13) introduced a deep learning method for CAD-RADS categorization, evaluating its performance on 288 single-center CCTA cases using 5-fold cross-validation. The study achieved a 3-category (CAD-RADS 0 *vs.* CAD-RADS 1–2 *vs.* CAD-RADS 3–5) accuracy of 60%, while that for 2 binary categories of CAD-RADS 0 *vs.* CAD-RADS >0 and CAD-RADS 0–2 *vs.* CAD-RADS 3–5 was 86% and 71%, respectively. In a recent international multicenter study, Lin

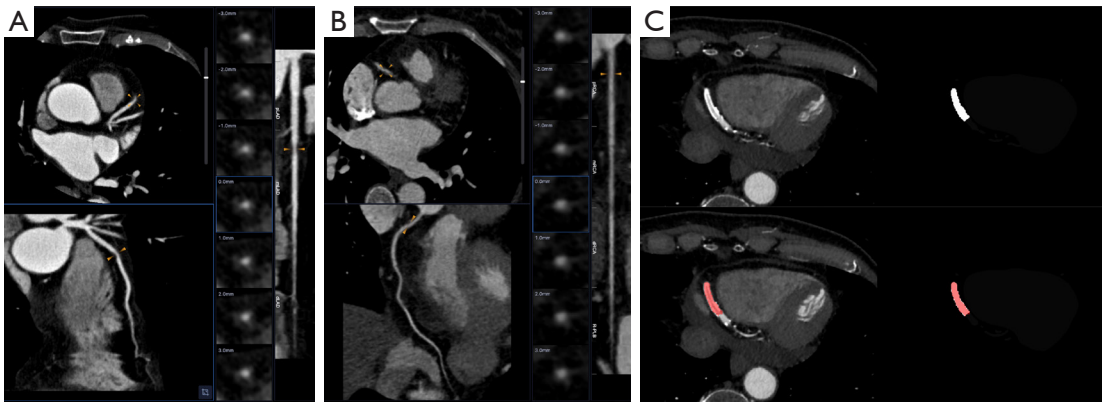

Figure 3 Example cases of the AI-based CAD-RADS categorization and stent segmentation. (A) A 69-year-old female with an LAD stenosis severity of CAD-RADS 3: axial view (top left), curved multiplanar reformatted image (bottom left), multiplanar along the centerline (second from right), and straightened MPR (right). AI identified a 54% stenosis (orange arrowheads) in the middle vessel segment. (B) A 57-year-old female with an RCA stenosis severity of CAD-RADS 1: axial view (top left), curved multiplanar reformatted image (bottom left), multiplanar along the centerline (second from right), and straightened MPR (right). AI identified a 19% stenosis (orange arrowheads) in the proximal vessel segment. (C) A 79-year-old male with a stent in the distal RCA: axial view of CCTA (top left), reference standard for stent volume (top right), AI-based stent segmentation prediction on CCTA (bottom left), and AI-based prediction compared to the reference standard (bottom right). AI, artificial intelligence; CAD-RADS, Coronary Artery Disease Reporting and Data System; LAD, left anterior descending artery; RCA, right coronary artery; MPR, multiplanar reformatted; CCTA, coronary computed tomography angiography.

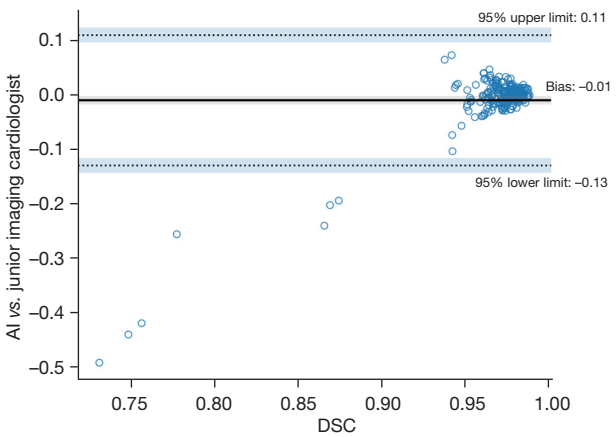

Figure 4 Bland-Altman plots demonstrated strong numerical agreement between the AI-assisted analysis system and junior imaging cardiologist, with a mean difference in DSC of −0.01 (95% CI limits of agreement ranging from −0.13 to 0.11). AI, artificial intelligence; DSC, Dice similarity coefficient; CI, confidence interval.

et al. (24) developed a hierarchical convolutional long short-term memory (ConvLSTM) network for rapid, automated plaque quantification of CCTA. This method exhibited strong agreement with expert readers and intravascular ultrasound, demonstrating prognostic value for future myocardial infarction.

Another crucial aspect in this field is the validation research of AI-assisted analysis products, which is essential for integrating AI into real-world clinical settings. Choi *et al.* (14) conducted the first confirmatory study of an FDA-approved AI product for CCTA. The AI-assisted approach to CCTA interpretation showed close agreement with expert readers in identifying coronary stenosis and CAD-RADS categories. Subsequently, the AI product's performance was further validated using data from 303 patients in a prospective, multicenter diagnostic derivation-validation, controlled clinical trial. The study reported high diagnostic performance for severe stenoses at both the ≥50% and ≥70% levels, along with a strong correlation with invasive quantitative coronary angiography (QCA) (25). Our findings suggest that the AI-based CCTA analysis method can offer rapid and accurate diagnoses of severe stenosis. At the per-patient level, our AI system demonstrated superior performance in detecting ≥50% stenosis and further improvement in identifying ≥70% stenosis. For per-vessel level stenosis diagnosis, the system exhibited high specificity and satisfactory sensitivity. In both the internal and external dataset, the AI's diagnosis of CAD-RADS categorization yielded a Cohen's kappa coefficient of at least 0.7 when

compared to the reference standard, and the agreement within 1 category was no lower than 95%. Notably, the average execution time for this AI system was under 5 min, while the standard-of-care workflow requires approximately 40 min for radiologists to draft a report.

As PCI technology evolves and progresses, postoperative stent follow-up is becoming a key function of CCTA. Along with assessing stent deformation and fracture, it is crucial to address ISR, a significant factor affecting the prognosis of patients with CAD. Consequently, automated stent identification is essential for AI-based comprehensive CCTA analysis. Our AI-assisted system displayed notably excellent performance in automated coronary stent segmentation, achieving a DSC of up to 0.96, on par with that of the junior imaging cardiologists.

We examined cases in which the AI system's stenosis severity assessment deviated from expert consensus on a per-vessel basis. First, we found that the AI system tended to overestimate the severity of CAD-RADS 0 vessel stenosis, primarily due to its high sensitivity, resulting in misjudgment of poor or heterogeneous lumen opacification. Second, for vessels with stenosis, the most frequent discordant cases occurred between CAD-RADS 1 and CAD-RADS 2, constituting 31.3% of disagreements in the internal dataset and 22.8% in the external dataset; this was followed by CAD-RADS 2 *vs.* CAD-RADS 3, with 29.1% in the internal dataset and 16.5% in the external dataset. Given that CAD-RADS scores represent discretized continuous stenosis severity values, interclass distances are subtle and susceptible to noise in training set labels. These challenges affect algorithm development, primarily impacting performance within the CAD-RADS 1–3 range. Finally, it is unsurprising that the AI system produced more cases of severe inconsistency in the external dataset. The agreement within 1 category was 99.0% for the internal dataset and 96.2% for the external dataset. The heterogeneity of imaging data represents the most significant limitation to the widespread application of AI systems in clinical practice, as it can profoundly degrade algorithm performance on unseen data.

This study has several limitations. First, the CAD-RADS categorization in this study was established through consensus among imaging cardiologists rather than through invasive examinations, such as invasive coronary angiography (ICA). This might have resulted in ground truth errors and hindered accurate calculation of the AI-assisted analysis system's performance concerning stenosis severity quantification. An important future work should involve collecting as much ICA data as possible to achieve a more accurate and comprehensive performance evaluation of the AI-assisted analysis systems. Second, the study primarily assessed the AI-assisted system's ability to quantify stenosis severity without examining other CAD-related indicators, such as plaque volume and type. Third, MPR is not sufficient for stenosis severity quantification. The AI-assisted analysis system used in this study solely employs MPR images for stenosis severity quantification in its deep learning model, which may result in suboptimal performance in certain instances. Our future work plans to take MPR images and cross-sectional images concurrently as input, integrating multiview information to improve the performance of the deep learning model. Fourth, we did not evaluate the performance of imaging cardiologists when supported by the AI system. Future research will investigate the role of AI-assisted analysis systems for imaging cardiologists with varying experience levels, focusing on both diagnostic performance and efficiency.

Conclusions

In summary, our multicenter study evaluated an AI-assisted analysis system for stenosis quantification and stent segmentation using CCTA scans. The AI-based method demonstrated superior performance in stenosis quantification, CAD-RADS categorization, and stent segmentation, with an average execution time of under 5 minutes. The system can potentially be integrated into routine workflows as a clinical decision support tool, assisting imaging cardiologists in enhancing the accuracy and efficiency of CCTA analysis.

Acknowledgments

Funding: None.

Footnote

Reporting Checklist: The authors have completed the STARD reporting checklist. Available at https://qims.amegroups.com/article/view/10.21037/qims-23-423/rc

Conflicts of Interest: All authors have completed the ICMJE uniform disclosure form (available at https://qims.amegroups.com/article/view/10.21037/qims-23-423/coif). PY, SY, XL, HZ, YW, HS, RZ and QZ are employed by Infervision Medical Technology Co., Ltd. The other

authors have no conflicts of interest to declare.

Ethical Statement: The authors are accountable for all aspects of the work in ensuring that questions related to the accuracy or integrity of any part of the work are appropriately investigated and resolved. The study was conducted in accordance with the Declaration of Helsinki (as revised in 2013) and was approved by institutional board of The Affiliated Chuzhou Hospital of Anhui Medical University. Individual consent for this retrospective analysis was waived.

References

1. GBD 2017 Causes of Death Collaborators. Global, regional, and national age-sex-specific mortality for 282 causes of death in 195 countries and territories, 1980-2017: a systematic analysis for the Global Burden of Disease Study 2017. Lancet 2018;392:1736-88.
2. Narula J, Chandrashekhar Y, Ahmadi A, Abbara S, Berman DS, Blankstein R, Leipsic J, Newby D, Nicol ED, Nieman K, Shaw L, Villines TC, Williams M, Hecht HS. SCCT 2021 Expert Consensus Document on Coronary Computed Tomographic Angiography: A Report of the Society of Cardiovascular Computed Tomography. J Cardiovasc Comput Tomogr 2021;15:192-217.
3. Choi AD, Geske JB, Lopez-Mattei JC, Parwani P, Wang DD, Winchester DE, Sengupta PP, Zoghbi WA, Shaw LJ, Chandrashekhar YS, Blankstein R. Cardiovascular Imaging Through the Prism of Modern Metrics. JACC Cardiovasc Imaging 2020;13:1256-69.
4. Newby DE, Adamson PD, Berry C, Boon NA, Dweck MR, Flather M, Forbes J, Hunter A, Lewis S, MacLean S, Mills NL, Norrie J, Roditi G, Shah ASV, Timmis AD, van Beek EJR, Williams MC. Coronary CT Angiography and 5-Year Risk of Myocardial Infarction. N Engl J Med 2018;379:924-33.
5. Knuuti J, Wijns W, Saraste A, Capodanno D, Barbato E, Funck-Brentano C, et al. 2019 ESC Guidelines for the diagnosis and management of chronic coronary syndromes. Eur Heart J 2020;41:407-77.
6. Cury RC, Abbara S, Achenbach S, Agatston A, Berman DS, Budoff MJ, Dill KE, Jacobs JE, Maroules CD, Rubin GD, Rybicki FJ, Schoepf UJ, Shaw LJ, Stillman AE, White CS, Woodard PK, Leipsic JA. Coronary Artery Disease - Reporting and Data System (CAD-RADS): An Expert Consensus Document of SCCT, ACR and NASCI: Endorsed by the ACC. JACC Cardiovasc Imaging 2016;9:1099-113.
7. Xie JX, Cury RC, Leipsic J, Crim MT, Berman DS, Gransar H, et al. The Coronary Artery Disease-Reporting and Data System (CAD-RADS): Prognostic and Clinical Implications Associated With Standardized Coronary Computed Tomography Angiography Reporting. JACC Cardiovasc Imaging 2018;11:78-89.
8. Nakanishi R, Motoyama S, Leipsic J, Budoff MJ. How accurate is atherosclerosis imaging by coronary computed tomography angiography? J Cardiovasc Comput Tomogr 2019;13:254-60.
9. Lu MT, Meyersohn NM, Mayrhofer T, Bittner DO, Emami H, Puchner SB, Foldyna B, Mueller ME, Hearne S, Yang C, Achenbach S, Truong QA, Ghoshhajra BB, Patel MR, Ferencik M, Douglas PS, Hoffmann U. Central Core Laboratory versus Site Interpretation of Coronary CT Angiography: Agreement and Association with Cardiovascular Events in the PROMISE Trial. Radiology 2018;287:87-95.
10. Litjens G, Kooi T, Bejnordi BE, Setio AAA, Ciompi F, Ghafoorian M, van der Laak JAWM, van Ginneken B, Sánchez CI. A survey on deep learning in medical image analysis. Med Image Anal 2017;42:60-88.
11. Dey D, Slomka PJ, Leeson P, Comaniciu D, Shrestha S, Sengupta PP, Marwick TH. Artificial Intelligence in Cardiovascular Imaging: JACC State-of-the-Art Review. J Am Coll Cardiol 2019;73:1317-35.
12. Zreik M, Lessmann N, van Hamersvelt RW, Wolterink JM, Voskuil M, Viergever MA, Leiner T, Išgum I. Deep learning analysis of the myocardium in coronary CT angiography for identification of patients with functionally significant coronary artery stenosis. Med Image Anal 2018;44:72-85.
13. Muscogiuri G, Chiesa M, Trotta M, Gatti M, Palmisano V, Dell'Aversana S, et al. Performance of a deep learning algorithm for the evaluation of CAD-RADS classification with CCTA. Atherosclerosis 2020;294:25-32.
14. Choi AD, Marques H, Kumar V, Griffin WF, Rahban

H, Karlsberg RP, Zeman RK, Katz RJ, Earls JP. CT Evaluation by Artificial Intelligence for Atherosclerosis, Stenosis and Vascular Morphology (CLARIFY): A Multi-center, international study. J Cardiovasc Comput Tomogr 2021;15:470-6.
15. Zreik M, van Hamersvelt RW, Wolterink JM, Leiner T, Viergever MA, Isgum I. A Recurrent CNN for Automatic Detection and Classification of Coronary Artery Plaque and Stenosis in Coronary CT Angiography. IEEE Trans Med Imaging 2019;38:1588-98.
16. Xu C, Guo H, Xu M, Duan M, Wang M, Liu P, Luo X, Jin Z, Liu H, Wang Y. Automatic coronary artery calcium scoring on routine chest computed tomography (CT): comparison of a deep learning algorithm and a dedicated calcium scoring CT. Quant Imaging Med Surg 2022;12:2684-95.
17. Wang W, Yang L, Wang S, Wang Q, Xu L. An automated quantification method for the Agatston coronary artery calcium score on coronary computed tomography angiography. Quant Imaging Med Surg 2022;12:1787-99.
18. Byrne RA, Serruys PW, Baumbach A, Escaned J, Fajadet J, James S, Joner M, Oktay S, Jüni P, Kastrati A, Sianos G, Stefanini GG, Wijns W, Windecker S. Report of a European Society of Cardiology-European Association of Percutaneous Cardiovascular Interventions task force on the evaluation of coronary stents in Europe: executive summary. Eur Heart J 2015;36:2608-20.
19. Dai T, Wang JR, Hu PF. Diagnostic performance of computed tomography angiography in the detection of coronary artery in-stent restenosis: evidence from an updated meta-analysis. Eur Radiol 2018;28:1373-82.
20. Abbara S, Blanke P, Maroules CD, Cheezum M, Choi AD, Han BK, Marwan M, Naoum C, Norgaard BL, Rubinshtein R, Schoenhagen P, Villines T, Leipsic J. SCCT guidelines for the performance and acquisition of coronary computed tomographic angiography: A report of the society of Cardiovascular Computed Tomography Guidelines Committee: Endorsed by the North American Society for Cardiovascular Imaging (NASCI). J Cardiovasc Comput Tomogr 2016;10:435-49.
21. Chen X, Wang X, Zhang K, Fung KM, Thai TC, Moore K, Mannel RS, Liu H, Zheng B, Qiu Y. Recent advances and clinical applications of deep learning in medical image analysis. Med Image Anal 2022;79:102444.
22. Ma X, Luo G, Wang W, Wang K. Transformer network for significant stenosis detection in CCTA of coronary arteries. Medical Image Computing and Computer Assisted Intervention–MICCAI 2021: 24th International Conference, Strasbourg, France, September 27–October 1, 2021, Proceedings, Part VI 24. Springer International Publishing; 2021:516-25.
23. Vaswani A, Shazeer N, Parmar N, Uszkoreit J, Jones L, Gomez AN, Kaiser Ł, Polosukhin I. Attention is all you need. Advances in neural information processing systems; 2017:30.
24. Lin A, Manral N, McElhinney P, Killekar A, Matsumoto H, Kwiecinski J, et al. Deep learning-enabled coronary CT angiography for plaque and stenosis quantification and cardiac risk prediction: an international multicentre study. Lancet Digit Health 2022;4:e256-65.
25. Griffin WF, Choi AD, Riess JS, Marques H, Chang HJ, Choi JH, et al. AI Evaluation of Stenosis on Coronary CTA, Comparison With Quantitative Coronary Angiography and Fractional Flow Reserve: A CREDENCE Trial Substudy. JACC Cardiovasc Imaging 2023;16:193-205.

Cite this article as: Meng Q, Yu P, Yin S, Li X, Chang Y, Xu W, Wu C, Xu N, Zhang H, Wang Y, Shen H, Zhang R, Zhang Q. Coronary computed tomography angiography analysis using artificial intelligence for stenosis quantification and stent segmentation: a multicenter study. Quant Imaging Med Surg 2023;13(10):6876-6886. doi: 10.21037/qims-23-423

Supplementary

Table S1 Detailed imaging acquisition information

Cohort and dataset	Scanner name	Number of scans	Type	KVP	In-plane pixel resolution (mm^2)
Internal Data-ISQ	GE HealthCare, Optima CT680 Series	9	Single-source, 64-row, 128-slice	100	0.38–0.49
	GE HealthCare, Revolution CT	110	Single-source, 256-row, 512-slice	100 or 120	0.36–0.59
	GE HealthCare, Revolution Maxima	26	Single-source, 64-row, 128-slice	100	0.49–0.53
	Philips Healthcare, iCT 256	67	Single-source, 128-row, 256-slice	120 or 140	0.33–0.56
	Philips Healthcare, Ingenuity Core 128	16	Single-source, 128-row, 256-slice	100 or 120	0.43–0.51
	Philips Healthcare, IQon Spectral CT	68	Double-source, 128-row, 256-slice	120	0.28–0.46
	Siemens Healthineers, SOMATOM Force	205	Double-source, 96-row, 192-slice	70, 80, 90, 100, 110, 120, 130	0.24–0.57
	Siemens Healthineers, SOMATOM Definition Flash	87	Double-source, 128-row, 256-slice	100 or 120	0.31–0.46
	Toshiba, Aquilion ONE	64	Single-source, 320-row, 640-slice	100 or 120	0.28–0.53
Internal Data-ISS	GE HealthCare, Optima CT680 Series	3	Single-source, 64-row, 128-slice	100	0.36–0.48
	GE HealthCare, Revolution CT	100	Single-source, 256-row, 512-slice	100 or 120	0.37–0.51
	GE HealthCare, Revolution Maxima	3	Single-source, 64-row, 128-slice	100	0.49
	Philips Healthcare, iCT 256	19	Single-source, 128-row, 256-slice	100 or 120	0.34–0.52
	Philips Healthcare, IQon Spectral CT	2	Double-source, 128-row, 256-slice	120	0.39
	Siemens Healthineers, SOMATOM Force	27	Double-source, 96-row, 192-slice	70, 80, 90, 100, 110, 120	0.27–0.43
	Siemens Healthineers, SOMATOM Definition Flash	45	Double-source, 128-row, 256-slice	100 or 120	0.34–0.47
	Toshiba, Aquilion ONE	36	Single-source, 320-row, 640-slice	100 or 120	0.31–0.49
External Data-ESQ	Siemens Healthineers, SOMATOM Drive	256	Double-source, 128-row, 256-slice	80, 100, 120	0.27–0.80

KVP, kilovolt peak; ISQ, internal stenosis quantification; ISS, internal stent segmentation; ESQ, external stenosis quantification.

https://dx.doi.org/10.21037/qims-23-423

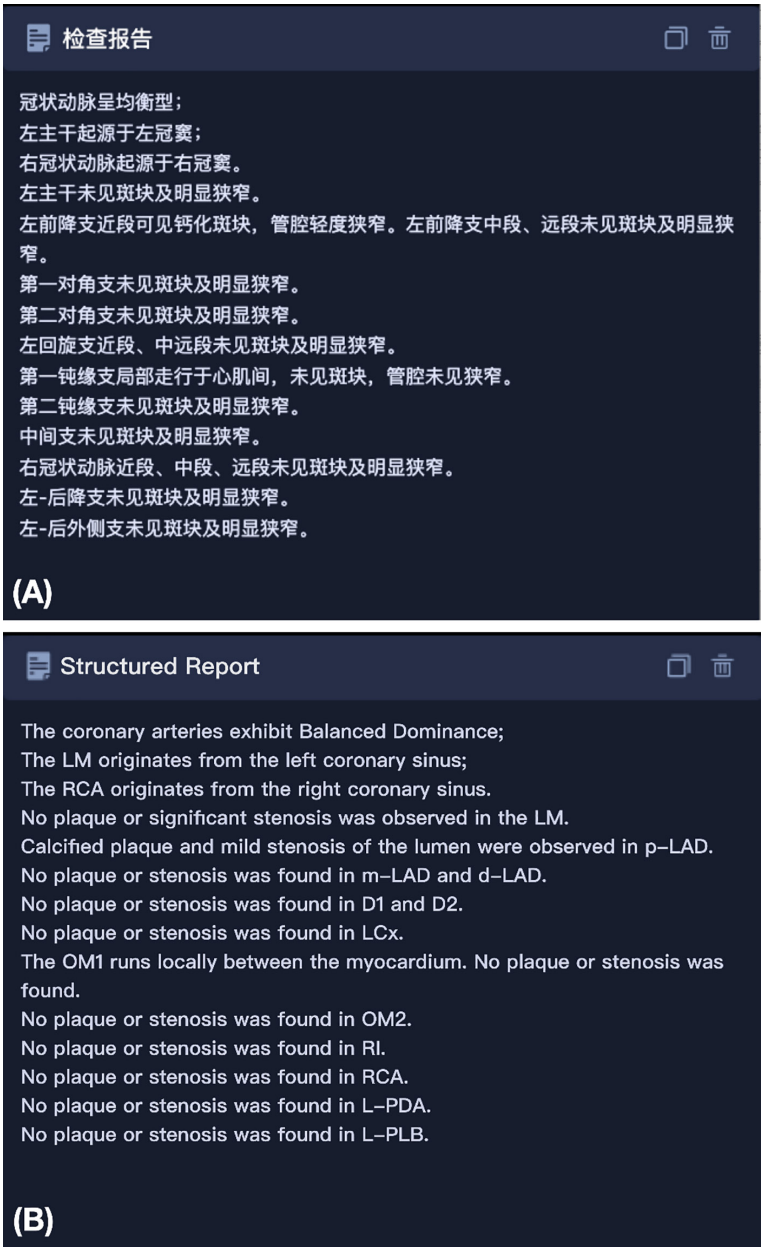

Figure S1 An AI-generated report example for a 73-old-year female with an LAD stenosis severity of CAD-RADS 2. (A) The content of AI-generated report, with the original Chinese version and (B) the corresponding English version. AI, artificial intelligence; CAD-RADS, Coronary Artery Disease Reporting and Data System; LM, left main artery; RCA, right coronary artery; LAD, left anterior descending artery; p-LAD, proximal-LAD; m-LAD, mid-LAD; d-LAD, distal LAD; D1, diagonal 1; D2, diagonal 2; LCx, left circumflex artery; OM1, obtuse marginal 1; OM2, obtuse marginal 2; RI, ramus intermedius; L-PDA, left posterior descending artery; L-PLB, left posterolateral branch.

https://dx.doi.org/10.21037/qims-23-423